



Cite this: *Phys. Chem. Chem. Phys.*,  
2015, 17, 24732

Received 1st May 2015,  
Accepted 7th July 2015

DOI: 10.1039/c5cp02549d

www.rsc.org/pccp

## Inverse internal conversion in $C_4^-$ below the electron detachment threshold

Naoko Kono,<sup>a</sup> Takeshi Furukawa,<sup>\*a</sup> Hajime Tanuma,<sup>a</sup> Jun Matsumoto,<sup>b</sup> Haruo Shiromaru,<sup>b</sup> Toshiyuki Azuma,<sup>c</sup> Kaveh Najafian,<sup>d</sup> Maria Susanne Pettersson,<sup>d</sup> Bertil Dynefors<sup>e</sup> and Klavs Hansen<sup>d</sup>

Inverse internal conversion followed by recurrent fluorescence was observed as a fast decay (10  $\mu$ s range) in the time profile of neutral yields from photo-excited  $C_4^-$  molecular ions. We also elucidated the contribution of such electronic radiative cooling to the  $C_4^-$  ions with internal energy far below the detachment threshold by an alternative novel approach, observing the laser wavelength and storage time dependence (ms range) of the total yield of the photo-induced neutrals.

### 1 Introduction

Carbon is the most abundant element in the universe, except for hydrogen, that can form molecules larger than dimers. Several carbon-rich molecules have been observed in space, including anions,<sup>1–3</sup> cations,<sup>4</sup> fullerenes,<sup>5</sup> and most lately iso-propyl cyanide,<sup>6</sup> emphasizing the need for laboratory data for the excitation and collision cross-section of these molecules and clusters. The composition of interstellar clouds, however, is also heavily influenced by the fate of the particles after excitation of light or after the rare collisions that build larger molecules.

In the dilute interstellar space, emission of radiation is the only means by which molecules, radicals and clusters can stabilize after excitation above the decomposition threshold. Radiative stabilization is important particularly for anions with their low activation energies for electron loss, and for small molecules with their small heat capacities. They are usually cooled by transitions between the vibrational levels by emission of infrared (IR) photons. We have observed that the de-excitation process of small carbon cluster anions,  $C_5^-$ ,  $C_7^-$ , and  $C_6H^-$ , is indeed well described by this scheme in experiments using the electrostatic ion storage ring, TMU E-ring.<sup>7–9</sup> In contrast, vibrationally hot  $C_6^-$  cools electronically, assisted by inverse internal conversion (IIC).<sup>9</sup> As schematically shown in Fig. 1, this is the process in which anions with a thermally populated electronic excited state emit visible or near IR photons. The rate of this process

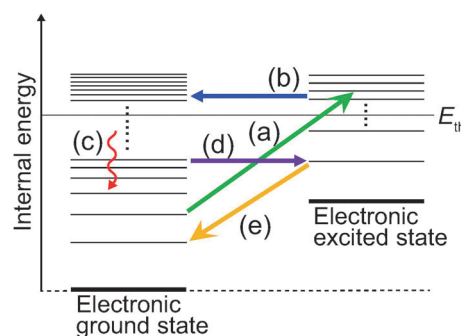


Fig. 1 Jablonski diagram of molecular anions with a low-lying electronic excited state. The arrows indicate the processes (a) electronic excitation, (b) internal conversion (IC), (c) vibrational radiative cooling, (d) inverse internal conversion (IIC), and (e) recurrent fluorescence.  $E_{th}$  stands for the electron detachment threshold (electron affinity of neutrals).

for  $C_6^-$  was measured with an electrostatic ion beam trap (EIBT).<sup>10</sup> The electronic cooling mechanism is also present for the larger anthracene cation, which is also a candidate molecule for the interstellar matter.<sup>11</sup>

In addition to the significance of the interstellar chemistry, the IIC process itself is of fundamental importance in molecular science, providing a good measure of the ergodic nature of photo-excited molecules. The theoretical study of IIC processes was initiated few decades ago,<sup>12</sup> and their presence was suggested by the observation of IR multiphoton-induced fluorescence,<sup>13</sup> but the observation was disputed.<sup>14</sup> The IIC processes of molecular ions were predicted theoretically, and a significant role of the resulting fluorescence, termed as recurrent fluorescence (RF) or Poincaré fluorescence, in stabilizing interstellar ions was pointed out.<sup>15,16</sup> The ion storage rings and ion beam traps equipped with high-sensitivity detection systems have been instrumental in the unambiguous identification of IIC and RF processes.<sup>9–11</sup>

<sup>a</sup> Department of Physics, Tokyo Metropolitan University, 1-1 Minamiosawa, Hachioji-shi, Tokyo 192-0397, Japan. E-mail: takeshi@tmu.ac.jp

<sup>b</sup> Department of Chemistry, Tokyo Metropolitan University, 1-1 Minamiosawa, Hachioji-shi, Tokyo 192-0397, Japan

<sup>c</sup> Atomic, Molecular & Optical Physics Laboratory, RIKEN, 2-1, Hirosawa, Wako-shi, Saitama 351-0198, Japan

<sup>d</sup> Department of Physics, University of Gothenburg, 41296 Gothenburg, Sweden

<sup>e</sup> Applied Physics, Chalmers Technical University, 41296 Gothenburg, Sweden

The presence of low-lying optically active electronically excited states is essential for this fast radiative cooling. The process is naturally expected also for other even-numbered carbon cluster anions due to the similarity in the electronic level structures of these open-shell species. In this paper, we show that the photo-excited hot  $C_4^-$  de-excites efficiently by RF *via* the IIC process similar to  $C_6^-$ . Zhao *et al.* reported that the internal conversion (IC) of the  $C^2\Pi_u$  state of  $C_4^-$  is faster than 30 ns, based on the characteristic one-photon and two-photon detachment photoelectron spectra.<sup>17</sup> Thus,  $C_4^-$  is a good candidate for the observation of IIC in a small molecule.

IIC processes have so far been observed by the fast decrease of yields of neutrals after photo-excitation as a consequence of competing fast radiative cooling.<sup>9–11</sup> This approach is valid for the internal energy region where the detachment rate is not zero, namely above the electron detachment threshold ( $E_{th}$ ), and lower than, or comparable to, the electronic cooling rate. As is shown later, such a condition is satisfied in a very narrow energy range for  $C_4^-$ . On the other hand, the IIC is expected to be a ubiquitous phenomenon for excited anions with the internal energy even below  $E_{th}$ , as long as the internal energy is above that of the electronic excited state. In the subsequent sections we will present evidence of the IIC of  $C_4^-$  below  $E_{th}$ , as well as evidence of the quenching effect of IIC at energies above  $E_{th}$ .

## 2 Experimental

Hot carbon cluster ions were produced by laser ablation of a graphite disk with a pulsed Nd:YAG laser (532 nm) which created the clusters in vibrationally and rotationally highly excited states.<sup>8</sup> The anions were extracted from the ion source without mass selection and accelerated to 15 keV. The bunched ions with a pulse width of about 1  $\mu$ s for each mass component were injected into the TMU E-ring.<sup>18</sup> The circulation period of  $C_4^-$  was 31.6  $\mu$ s. The undesired ions, such as  $C_4H^-$ , were eliminated by the application of synchronized voltage pulses to a deflector electrode 0.3 ms or 0.4 ms after injection into the ring.

After a certain storage time (up to 14 ms), the stored ions were photo-excited using a tunable optical parametric oscillator (OPO) laser of a wavelength of 480–690 nm (2.58–1.80 eV) with a pulse duration below 10 ns. The adiabatic electron affinity  $E_{th}$  of  $C_4^-$  has been measured to be 3.88 eV,<sup>19</sup> which is above the photon energies used here. Since the decay requires an initial internal energy that contributes to the emission process, the detachment is most likely thermally driven. We detected the neutral products using a microchannel plate (MCP). These were neutral  $C_4$ , and dissociation products are excluded according to a previous report.<sup>20</sup>

As shown in Fig. 2(a), the laser pulse merged with the ion bunch in the straight section of the ring opposite to the side where the neutrals produced by the laser induced electron detachment were detected by the MCP. In this experimental configuration, the neutralized products were detected in a time window delayed relative to the laser irradiation by one-half revolution in the ring (after 15.8  $\mu$ s).

The electron detachment process due to two-photon absorption was not observed because the internal energy after two-photon

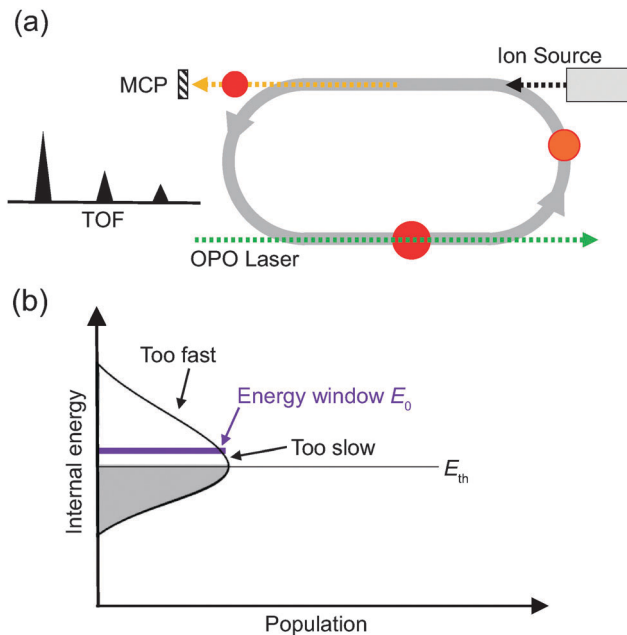


Fig. 2 (a) Schematics of the experimental setup. The ion bunches produced using the laser ablation ion source were stored in the ring and laser-irradiated at the straight section opposite to the ion injection side. The resulting neutral particles were detected with a MCP at the injection side section after circulating one-half revolution. (b) Generic energy distribution of photo-excited anions and energy regions relevant to the energy window concept. In the  $C_4^-$  case,  $E_0$  is calculated to be just above  $E_{th} = 3.88$  eV. And the width of the window is very narrow, with a FWHM of 1 meV for a half revolution after laser excitation. We can therefore set  $E_0 = E_{th}$  to a good approximation.

absorption is so high that the detachment occurs much faster than 15.8  $\mu$ s it takes before the anions enter the detection area in the ring. The one-photon detachment is further guaranteed by the fact that the neutralization yield was proportional to the laser power around the laser pulse energy employed in the present study, below 5 mJ per pulse.

Considering the fast IC observed for  $C_4^-$ ,<sup>17</sup> a delay time of 15.8  $\mu$ s is long enough to thermalize the excitation energy, namely to distribute it to the vibrational modes of the electronic ground and excited states. The observed laser induced neutral yield reflects the population in the specific internal energy region (the energy window  $E_0$ ) above  $E_{th}$  as illustrated in Fig. 2(b). This energy window is defined by the decay times determined by the experimental configuration and the fact that the delayed electron detachment rate ( $k_d$ ) varies rapidly with energy. For  $C_4^-$  in the present configuration,  $E_0$  is calculated to be just above  $E_{th} = 3.88$  eV, and the width of the window is very narrow, with a FWHM of 1 meV for a half revolution after laser excitation. We can therefore set  $E_0 = E_{th}$  to a good approximation.

## 3 Results and discussion

### 3.1 Theoretical description of the cooling processes of the photo-excited $C_4^-$

Theoretically calculated rates of delayed electron detachment ( $k_d$ ), RF photon emission ( $k_{RF}$ ), and IR photon emission ( $k_v$ ) are

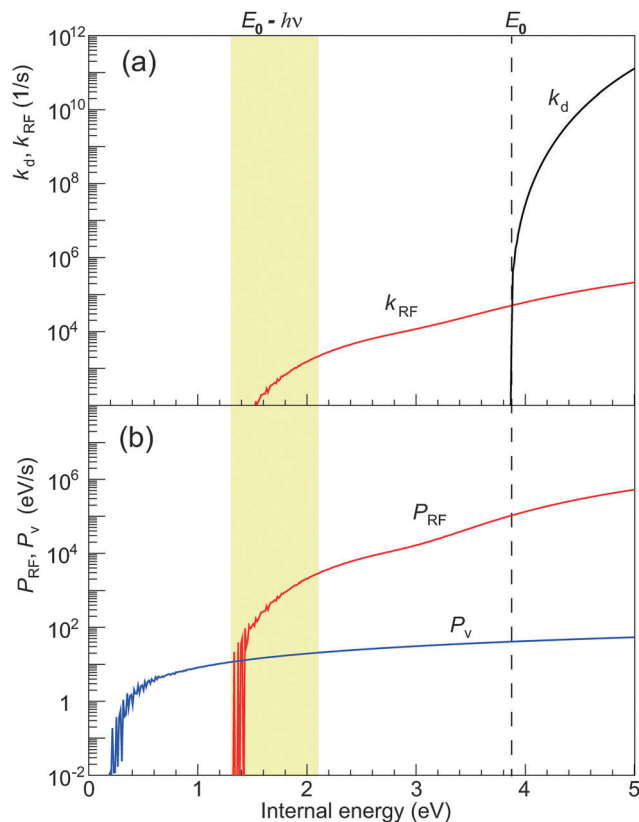


**Fig. 3** (a) Calculated detachment rate constant  $k_d$  (black line), and the recurrent fluorescence (RF) rate constant  $k_{\text{RF}}$  (red line) for  $\text{C}_4^-$  as a function of internal energy  $E$ . (b) Calculated electronic (in red) and vibrational (in blue) radiative cooling rates, namely the emitted energy (in eV) per second denoted as  $P_{\text{RF}}$  and  $P_v$ , respectively, of  $\text{C}_4^-$  as a function of the internal energy  $E$ . The dashed line shows the position of  $E_0$ , and the yellow area indicates the probed region of  $E_0 - h\nu$ , as explained below.

shown in Fig. 3 as a function of the total internal energy  $E$ . For convenience, we show rate constants ( $\text{s}^{-1}$ ) of  $k_d$  and  $k_{\text{RF}}$  in Fig. 3(a), and add a comparison of the radiative cooling rates, *i.e.*, emission energy rates ( $\text{eV s}^{-1}$ ), between RF and IR photon emissions in Fig. 3(b). The RF emission energy rate is expressed as  $P_{\text{RF}} = \sum_i E_{\text{RF}}^i k_{\text{RF}}^i$ , where  $E_{\text{RF}}^i$  and  $k_{\text{RF}}^i$  are the energy and transition rate of the  $i$ -th electronic excited state, while the IR emission energy rate is  $P_v = \sum_j h\nu_j k_v^j$ , where  $h\nu_j$  and  $k_v^j$  are the  $j$ -th vibrational transition energy and rate.

These rate constants were evaluated in the same manner as those for the  $\text{C}_6^-$  anion.<sup>9,21</sup> All are calculated with the detailed balance equations pertaining to the specific process.

For  $k_d$  the expression is

$$k_d(E) = \int_0^{E-E_{\text{th}}} \frac{2m}{\pi^2 \hbar^3} \sigma_c(\varepsilon) \varepsilon \frac{\rho_d(E - E_{\text{th}} - \varepsilon)}{\rho_p(E)} d\varepsilon, \quad (1)$$

where  $m$  is the mass of an electron,  $\varepsilon$  the kinetic energy of the emitted electron,  $\sigma_c$  the cross section of electron capture, *i.e.*, reversal process of electron emission,  $\rho$ 's the level densities of

the species given by the subscript  $p$  and  $d$  as that of the parent (anion) and the daughter (neutral), respectively. The numerical factor two in the formula is the spin degeneracy for the emitted electron while the electronic degeneracies of the parent and the daughter are included in their level densities. The required electron capture cross-section was tentatively assumed to be given by the Langevin equation with a neutral cluster polarizability of 52.6 a.u.<sup>22</sup> In eqn (1) and the following procedure, all vibrations are assumed to be harmonic. The vibrational level densities were calculated using the Beyer-Swinehart algorithm<sup>23</sup> with the frequencies for  $\text{C}_4^-$  and  $\text{C}_4$  given in ref. 24 and 25. Integration over  $\varepsilon$  was performed numerically with a step of  $1 \text{ cm}^{-1}$ . The curves in Fig. 3 show the values averaged over  $100 \text{ cm}^{-1}$ .

The vibrational cooling rate was calculated from the vibrational transition rates of the  $j$ -th vibrational mode  $k_v^j$ , as

$$k_v^j(E) = A_{1-0}^j \frac{1}{\rho(E)} \sum_n n \rho_j(E - nh\nu_j), \quad (2)$$

where  $A_{1-0}^j$  is the Einstein A-coefficient,  $\rho$  is the level density taking account of all the vibrational modes,  $\rho_j$  are those without the  $j$ -th vibrational mode, and  $n$  is the vibrational quantum number.<sup>21</sup> The A-coefficients used in the simulation were those given in ref. 24.

The states relevant for RF are known;  $\text{X}^2\Pi_g$  (the ground state),  $\text{A}^2\Sigma_g^+$  (the energy of the excited state  $E_{\text{RF}} = 1.00 \text{ eV}$ ),  $\text{B}^2\Sigma_u^+$  ( $E_{\text{RF}} = 1.34 \text{ eV}$ ) and  $\text{C}^2\Pi_u$  ( $E_{\text{RF}} = 2.71 \text{ eV}$ ).<sup>26,27</sup> The transition between the A state and the ground state is forbidden, and A-coefficients for the B state and the C state are calculated to be  $4.7 \times 10^5 \text{ s}^{-1}$  and  $1.3 \times 10^7 \text{ s}^{-1}$ , respectively.<sup>28,29</sup> This RF mechanism is active when the internal energy is above  $E_{\text{RF}}^i$ , and proceeds with the rate constant, expressed in terms of the A-coefficient,

$$k_{\text{RF}}^i(E) = A_i \frac{\rho(E - E_{\text{RF}}^i)}{\rho(E)}. \quad (3)$$

### 3.2 Decay time-profile of the photo-excited $\text{C}_4^-$

Examples of a time trace with and without laser excitation at 5.012 ms are shown in Fig. 4. Without laser excitation, a periodic train of low intensity peaks of neutral counts was observed as a background, reflecting the circulation period of  $31.6 \mu\text{s}$ . This background was due to collisions with residual gas molecules in the ring, and it decreased exponentially with a time constant on the order of a second. After laser irradiation, a strong enhancement of the neutral yield was observed.

Fig. 5 shows the neutralization yields at 0.5, 1.5 and 2.5 revolutions after excitation with a single photon of 355 nm (3.49 eV, circles), 480 nm (2.58 eV, squares), both for a storage time of 5 ms, and 480 nm at a storage time of 0.5 ms (crosses). The yields are normalized to the value at 0.5 revolutions.

The electronic radiative cooling is far stronger than the vibrational cooling, and the latter is negligibly small at the internal energy around  $E_0 = 3.88 \text{ eV}$ , as seen in Fig. 3(b). Electron detachment (and the associated depletion cooling)

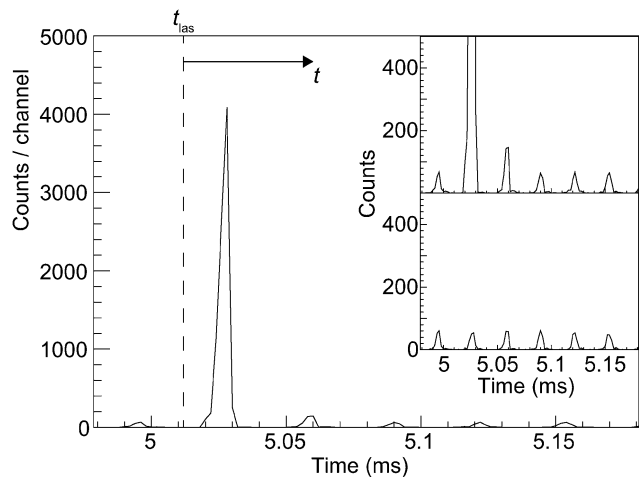


Fig. 4 The neutral yield at  $\lambda = 480$  nm ( $h\nu = 2.58$  eV) and a laser firing time ( $t_{\text{las}}$ ) of 5.012 ms. The top inset shows an expanded view of the same time interval, showing the enhanced first and second peaks following laser excitation. The lower inset shows a reference spectrum recorded without laser pulses.

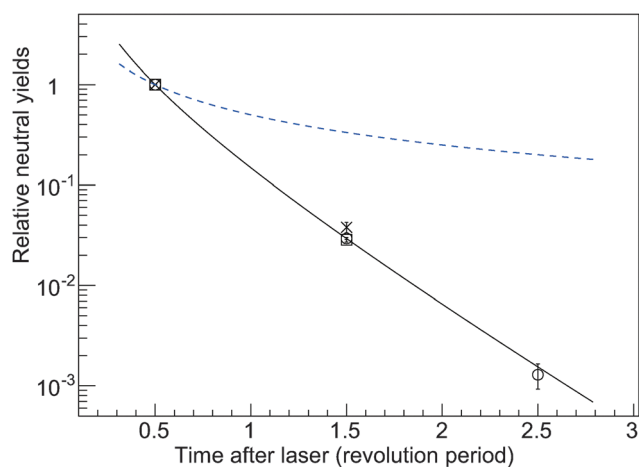


Fig. 5 Neutral yields versus time after excitation with a single photon of 355 nm (3.49 eV) at 5 ms storage (circles), and 480 nm (2.58 eV) at 5 ms (squares) and 0.5 ms storage (crosses). The plots are normalized at a storage time of 0.5 revolutions. At 1.5 revolutions, the three data points coincide. At 2.5 revolutions only the wavelength 355 nm gave a statistically significant signal. The dashed blue line shows the  $1/t$  decay (power law), and the solid black line is a fit of eqn (6).

and the radiative electronic cooling compete around  $E_0$  and give the neutral yield

$$I(t) \propto \int_{E_{\text{th}}}^{\infty} g(E - h\nu) k_d(E) e^{-\{k_d(E) + k_{\text{RF}}(E)\}t} dE, \quad (4)$$

The electronic cooling by  $k_{\text{RF}}$  is treated as discrete, because the energy taken away by a single decay will place the energy far below  $E_0 - h\nu$ . Since both  $k_{\text{RF}}(E)$  and  $g(E - h\nu)$  vary much slower with internal energy than does  $k_d(E)$ , they can be approximated by  $k_{\text{RF}}(E_0)$  and  $g(E_0 - h\nu)$ , respectively, and factored out from the integral,

$$I(t) \approx e^{-k_{\text{RF}}(E_0)t} g(E_0 - h\nu) \int_{E_{\text{th}}}^{\infty} k_d(E) e^{-k_d(E)t} dE. \quad (5)$$

When no radiative cooling occurs,  $I(t)$  is given by the last integral in eqn (5) which integrates to a power law in time (prop.  $1/t$ ), as has been discussed in detail elsewhere.<sup>30</sup> Then

$$I(t) \propto e^{-k_{\text{RF}}(E_0)t}/t. \quad (6)$$

The decay profiles of the photo-induced neutral yield shown in Fig. 5 are clearly fast compared with the ion circulation period of 31.6  $\mu\text{s}$ , and the decay is measured over three orders of magnitude for the three data points (0.5, 1.5 and 2.5 revolutions after laser excitation). The energy windows corresponding to 1.5 and 2.5 revolutions after excitation are almost the same as  $E_0$ . The fast, almost exponential, decay stands in sharp contrast to the photon-enhanced decays for species described by the power law where the electronic radiative cooling mechanism is absent. The measured points were fitted with eqn (6) and gave the value  $k_{\text{RF}} = 7.7 \times 10^4 \text{ s}^{-1}$  at  $E_0 = E_{\text{th}} = 3.88$  eV. This value will be discussed below.

### 3.3 Storage time dependence of the yield of the photo-excited $\text{C}_4^-$

As can be seen in Fig. 3, RF is expected to be a major cooling pathway in a wide energy region below  $E_{\text{th}}$ . To measure  $k_{\text{RF}}$  in this energy region, instead of analyzing the detachment time profile after photo-excitation, it is useful to study the population before photo-excitation, and its time evolution as a function of  $E_0 - h\nu$ . The measured signal at  $E_0$  immediately after laser irradiation of the energy  $h\nu$  is proportional to the population at  $E_0 - h\nu$  before the laser irradiation. From the ion storage time dependence, we can therefore get information on the time development of the population at  $E_0 - h\nu$ , namely  $g(E_0 - h\nu, t_{\text{las}})$ , where  $t_{\text{las}}$  is the laser firing time. By changing  $h\nu$ , we can survey a wide range of internal energies.

Fig. 6(a) shows the  $t_{\text{las}}$  dependence for 480, 500, 530/532, 580, 620, 650, 680 and 690 nm laser irradiation corresponding to the sampling internal energy of  $E_0 - h\nu$  from 1.30 to 2.08 eV as shown in Fig. 3. The yield was found to decrease monotonically with the ion storage time before laser irradiation. A striking feature is that the yield started decreasing significantly (more than 10 times) faster with the storage time for the excitation energy above the energy level of the  $\text{B}^2\Sigma_u^+$  state (1.34 eV), indicating that the ions in this energy region are cooled by the RF from the B state.

As for the minor contribution of IR cooling, Fig. 3(b) shows that IR emission corresponds to photon emission rates from 10  $\text{eV s}^{-1}$  (at the internal energy  $E_0 - h\nu = 1.30$  eV) to 20  $\text{eV s}^{-1}$  (at  $E_0 - h\nu = 2.08$  eV). This is 0.14 eV for the longest (14 ms) measurement at 480 nm, and 0.02 eV for 1 ms at 690 nm in Fig. 6(a). Since the possible energy shift by IR emission in this time region is much smaller than the spread of the internal energies, the cooling by RF is the only means of considerable changes in population at  $E_0 - h\nu$ . In contrast to the IR cooling, in which the population at  $E_0 - h\nu$  is given by the balance of incoming and outgoing components, the RF cooling does not involve incoming components since the energy removed by a single transition is too large, allowing us to adopt the following approximation,

$$I(t_{\text{las}}) \propto g(E_0 - h\nu, t_{\text{las}}) = e^{-k_{\text{RF}}(E_0 - h\nu)t_{\text{las}}} g(E_0 - h\nu, t_{\text{las}} = 0). \quad (7)$$

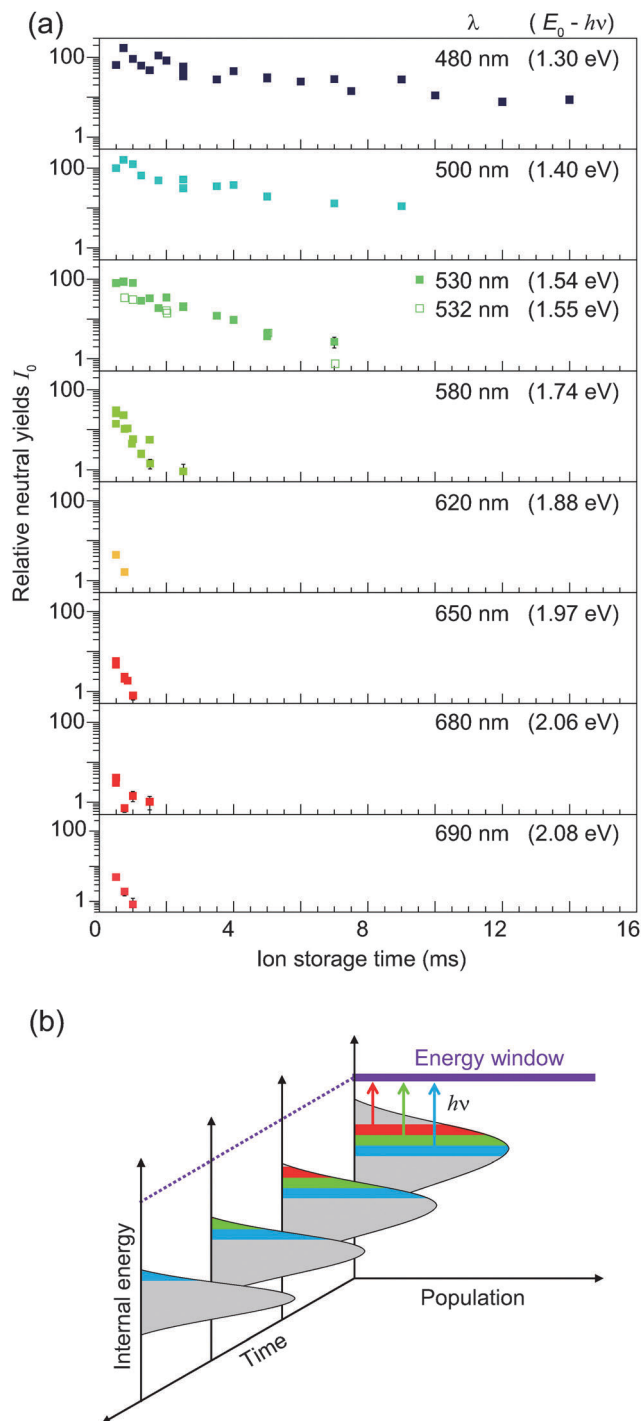


Fig. 6 (a) The relative neutral yields as a function of the ion storage time before laser irradiation at different photon energies. The yields were normalized by the averaged yield during 15 revolutions prior to the laser pulse injection. (b) Schematics of the evolution of the sampled population during the cooling process.

This expression for a first-order reaction is consistent with the near-exponential profiles in the 10 ms range seen in Fig. 6(a). The fitted values of  $k_{\text{RF}}(E_0 - h\nu)$  are plotted in Fig. 7 as a function of the sampled energy of  $E_0 - h\nu$ . We compare these rates with the calculated  $k_{\text{RF}}$  (already shown in Fig. 3(a) derived from eqn (3)).

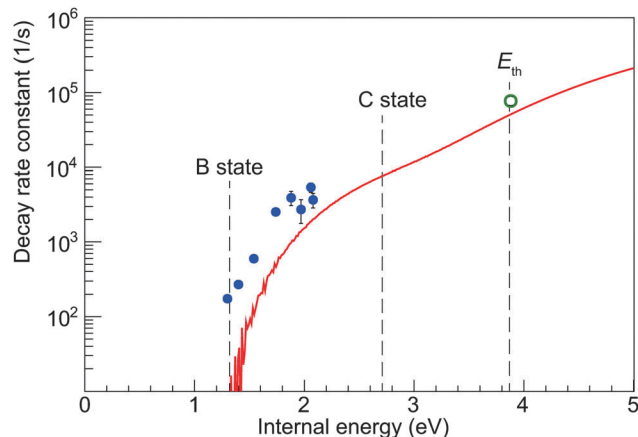


Fig. 7 Calculated recurrent fluorescence (RF) rate constant  $k_{\text{RF}}$  for  $\text{C}_4^-$  as a function of the internal energy  $E$  (red line) (the same as in Fig. 3(a)). Experimental RF rate constants obtained from the storage time dependence (filled blue circles) and those from the decay time-profile (open green circle) are also shown. The vertical dashed lines give the energies of the B state (1.34 eV), the C state (2.71 eV) and  $E_{\text{th}}$  (3.88 eV). Transitions from the A state (1.00 eV) are forbidden.

The observed cooling rates agree surprisingly well with our calculated electronic cooling rate. Note that, depending on the values of the two  $A$ -coefficients, the overall curve may shift up or down but the energy dependence would not change qualitatively, and the threshold behavior would only change very little. We consider the agreement very satisfactory. This fact provides strong evidence for the presence of the IIC process far below the detachment threshold.

Then, we plotted the value of  $7.7 \times 10^4 \text{ s}^{-1}$  extracted from the decay time-profile at the internal energy of  $E_0$  for comparison in Fig. 7. It is again in good agreement with our calculation. We also noticed that this value is very close to the theoretical estimate reported by Terzieva *et al.*<sup>31</sup>

## 4 Conclusions

We have demonstrated that the photo-excited hot  $\text{C}_4^-$  ions de-excite efficiently by recurrent fluorescence (RF) following inverse internal conversion (IIC). This electronic radiative cooling process was observed by two complementary approaches. The analysis of the fast decay time profile after photo-excitation was valid for  $E > E_{\text{th}}$ , whereas the total yield analysis at various photon energies and the ion storage times, *i.e.*, laser firing times was valid for  $E < E_{\text{th}}$ .

From an astrochemical point of view, the stability of the small hydrocarbon anions, such as  $\text{C}_{2n}\text{H}^-$  ( $n = 2-4$ ), has been a hot topic. Prevented by the difficulty in detection by the rotational transitions, chain-form carbon cluster anions,  $\text{C}_n^-$ , have not been identified in space. However, they must be abundant in the interstellar clouds. These ions are expected to be produced in collisions of the neutral molecule and an electron, and their stability is determined by the competition between radiative cooling and electron detachment. Our observation of the fast radiative cooling suggests that  $\text{C}_4^-$  has a chance to survive the electron detachment.

## Acknowledgements

This work was supported by the Swedish Foundation for International Cooperation in Research and Higher Education (STINT) and the Swedish Royal Academy. It was also supported by JSPS KAKENHI Grant Number 26220607. We thank Dr Kaito Takahashi and Dr Zexing Cao for independently providing us their results of theoretical calculations.

## References

- 1 M. C. McCarthy, C. A. Gottlieb, H. Gupta and P. Thaddeus, *Astrophys. J.*, 2006, **652**, L141–L144.
- 2 M. Agúndez, J. Cernicharo, M. Guélin, M. Gerin, M. C. McCarthy and P. Thaddeus, *Astron. Astrophys.*, 2008, **478**, L19–L22.
- 3 S. Brünken, H. Gupta, C. A. Gottlieb, M. C. McCarthy and P. Thaddeus, *Astrophys. J.*, 2007, **664**, L43–L46.
- 4 A. G. G. M. Tielens, *Rev. Mod. Phys.*, 2013, **85**, 1021–1081.
- 5 J. Cami, J. Bernard-Salas, E. Peeters and S. E. Malek, *Science*, 2010, **329**, 1180–1182.
- 6 A. Belloche, R. T. Garrod, H. S. P. Müller and K. M. Menten, *Science*, 2014, **345**, 1584–1587.
- 7 M. Goto, A. E. K. Sundén, H. Shiromaru, J. Matsumoto, H. Tanuma, T. Azuma and K. Hansen, *J. Chem. Phys.*, 2013, **139**, 054306.
- 8 K. Najafian, M. S. Pettersson, B. Dynefors, H. Shiromaru, J. Matsumoto, H. Tanuma, T. Furukawa, T. Azuma and K. Hansen, *J. Chem. Phys.*, 2014, **140**, 104311.
- 9 G. Ito, T. Furukawa, H. Tanuma, J. Matsumoto, H. Shiromaru, T. Majima, M. Goto, T. Azuma and K. Hansen, *Phys. Rev. Lett.*, 2014, **112**, 183001.
- 10 V. Chandrasekaran, B. Kafle, A. Prabhakaran, O. Heber, M. Rappaport, H. Rubinstein, D. Schwalm, Y. Toker and D. Zajfman, *J. Phys. Chem. Lett.*, 2014, **5**, 4078–4082.
- 11 S. Martin, J. Bernard, R. Bredy, B. Concina, C. Joblin, M. Ji, C. Ortega and L. Chen, *Phys. Rev. Lett.*, 2013, **110**, 063003.
- 12 A. Léger, P. Boissel and L. d'Hendecourt, *Phys. Rev. Lett.*, 1988, **60**, 921.
- 13 Z. Karny, A. Gupta, R. Zare, J. N. ST. Lin and A. Ronn, *Chem. Phys.*, 1979, **37**, 15–20.
- 14 J. Y. Tsao, N. Bloembergen and I. Burak, *J. Chem. Phys.*, 1981, **75**, 1–8.
- 15 A. Nitzan and J. Jortner, *J. Chem. Phys.*, 1979, **71**, 3524–3532.
- 16 E. Herbst and Y. Osamura, *Astrophys. J.*, 2008, **679**, 1670–1679.
- 17 Y. Zhao, E. de Beer, C. Xu, T. Taylor and D. M. Neumark, *J. Chem. Phys.*, 1996, **105**, 4905–4919.
- 18 S. Jinno, T. Takao, K. Hanada, M. Goto, K. Okuno, H. Tanuma, T. Azuma and H. Shiromaru, *Nucl. Instrum. Methods Phys. Res., Sect. A*, 2007, **572**, 568–579.
- 19 D. W. Arnold, S. E. Bradforth, T. N. Kitsopoulos and D. Neumark, *J. Chem. Phys.*, 1991, **95**, 8753–8764.
- 20 B. Pozniak and R. C. Dunbar, *Int. J. Mass Spectrom. Ion Processes*, 1994, **133**, 97–110.
- 21 T. Furukawa, G. Ito, M. Goto, T. Majima, H. Tanuma, J. Matsumoto, H. S. K. Hansen and T. Azuma, *Nucl. Instrum. Methods Phys. Res., Sect. B*, 2015, **354**, 192.
- 22 P. Fuentealba, *Phys. Rev. A: At., Mol., Opt. Phys.*, 1998, **58**, 4232.
- 23 T. Beyer and D. F. Swinehart, *Commun. ACM*, 1973, **16**, 379.
- 24 J. Szczepanski, S. Ekern and M. Vala, *J. Phys. Chem. A*, 1997, **101**, 1841–1847.
- 25 J. M. L. Martin, *J. Phys. Chem.*, 1996, **100**, 6047–6056.
- 26 P. Freivogel, M. Grutter, D. Forney and J. P. Maier, *J. Chem. Phys.*, 1997, **107**, 22–27.
- 27 Y. Zhao, E. de Beer and D. M. Neumark, *J. Chem. Phys.*, 1996, **105**, 2575–2582.
- 28 Z. Cao, private communication.
- 29 K. Takahashi, private communication.
- 30 K. Hansen, J. U. Andersen, P. Hvelplund, S. P. Møller, U. V. Pedersen and V. V. Petrunin, *Phys. Rev. Lett.*, 2001, **87**, 123401.
- 31 R. Terzieva and E. Herbst, *Int. J. Mass Spectrom.*, 2000, **201**, 135–142.